Physica B 657 (2023) 414566

Contents lists available at ScienceDirect

Physica B: Condensed Matter

journal homepage: www.elsevier.com/locate/physb

Effect of thermal annealing on the electronic parameters of Al/p-Si/Cu double Schottky barrier heights

Mustafa Okutan [a,*], Andreas Bablich [b,**], Peter Haring Bolivar [a,***]

[a] Institute of High Frequency and Quantum Electronics, University of Siegen, D-57076, Siegen, Germany
[b] Institute of Graphene-based Nanotechnology, University of Siegen, D-57076, Siegen, Germany

ARTICLE INFO

Keywords:
Double Schottky diode
Interface state density
Ohmic contact
Current-voltage
Conductance-capacitance technique

ABSTRACT

In this work, performance enhancements of a double Schottky rectifier diode with Cu contact on top of p-type Si and a back-side-Al contact due to an optimized thermal annealing process are reported. A decrease of the ideality factor for non-ohmic and ohmic Schottky contacts from 3.17 to 1.15 could be observed in conjunction with a barrier height reduction from 0.59 eV to 0.48 eV by thorough hydrofluoric acid treatment prior to annealing the sample for 15 min. at 450 °C in N_2 atmosphere. Moreover, the barrier height and built-in voltage values decreased by increasing frequency in the ohmic contact structure. The results presented in this work demonstrate such ohmic contacts to be potential candidates for high current and low resistance Schottky diodes and applications.

1. Introduction

Metal-semiconductor-metal (MSM)/Schottky barrier (SB) diodes play a significant role for a huge variety of rectifier diode applications. It has been reported that the passivation effect of the native oxide layer gets lost, the surface defects change and the Schottky barrier height (SBH) increases due to annealing at high temperatures [1]. Au/p-CoS/n-Si/Al heterojunction devices produced by spray pyrolysis may act as solar cells as demonstrated in [2]. Here, diode parameters were determined in the dark state and under illumination conditions. Nonselective resistive switching memory cells were studied in a Ni/HfO_2/TiN high density crossbar array for the interface control in memory structures utilizing Schottky junction devices [3]. In principle, rectifying MS contacts are the most widely used SB junctions established in high frequency electronic devices [4]. Recently, GHz switching in silicon-based SB could be achieved [5]. Systematic electrical characterization studies on a huge variety of SB structures and material compositions have already been carried out by different groups. The effect of high-frequency bias pulses produced by diffusion parameters of a p-Si Schottky diode containing positively charged iron was demonstrated [6]. To investigate SB diode characteristics in terms of electrical properties, the structural properties of metals with different work functions (Mn, Cd, Al, Bi, Ph, Sn, Sb, Fe and Ni) have been exploited in combination with p-type Si semiconductors. Various SB diode parameters have been determined by the I–V technique for these nine metals with Schottky barrier heights varying between 0.56 eV (Fe) and 0.85 eV. Studies on the SB height for different metals and the influence on the diodes SBH and ideality factor in forward biasing conditions have also been conducted by Cankaya et al. [7]. A polycrystalline *n*-PbTe/p-GaP heterojunction was fabricated by electron beam deposition. It has been shown that thermal annealing enables significant improvements in the parameters of the polycrystalline junction diode verifying thermal post-processing to be an important heterojunction application process [8]. Radio frequency molecular beam epitaxy (MBE) thin film deposition has been utilized for the fabrication of a SB diode containting high temperature AlN as buffer layer for Mg-doped GaN on Si substrates. To shed light on photonic applications, electroluminescence properties were investigated by producing Mg-doped p-GaN films on Ni ohmic and Schottky contacts using In. Schottky and ohmic contact sides determined as cathode and anode, are examined as two Schottky joints. It has been demonstrated that these thin-film electroluminescent devices are associated with SBH [9]. Parameters, such as Al/p-Si Schottky rectifier diode interface states, variation of series resistor properties, barrier height and ideality factor are all investigated in Ref. [10]. It has been stated that the

* Corresponding author. High Frequency and Quantum Electronics, University of Siegen, D-57076, Siegen, Germany.
** Corresponding author. Graphene-based Nanotechnology, University of Siegen, D-57076, Siegen, Germany.
*** Corresponding author. High Frequency and Quantum Electronics, University of Siegen, D-57076, Siegen, Germany.
E-mail addresses: Mustafa.Okutan@uni-siegen.de (M. Okutan), andreas.bablich@uni-siegen.de (A. Bablich), peter.haring@uni-siegen.de (P. Haring Bolivar).

https://doi.org/10.1016/j.physb.2022.414566
Received 3 November 2022; Received in revised form 30 November 2022; Accepted 5 December 2022
Available online 7 December 2022

passivation process on the silicon surface increases the Schottky contact due to the oxide layer formation on top of the semiconductor. It was found that an initial pretreatment in hydrofluoric acid can change and precisely tune the interface states, and serial resistance values of p-Si/Al SBH [11]. Besides the SBH and the ideality factor, the built-in potential and the width of the depletion region play a significant role in tuning and optimizing the diode performance. Typical characterization methods to extract these parameters comprise frequency dependent conductance voltage and capacity-voltage techniques. Ohmic junctions typically obtain lower resistance values rather than that of the Schottky junctions, allowing non-linear current to flow in only one direction [12–15]. Such measurements have been applied to study diode properties of Al/perylene/p-Si Schottky junctions [16]. In experimental observations of different Schottky diodes, the absence and presence of intermediate regions strongly determines the electrical device behavior. In this sense, the values obtained when the capacitance-voltage changes of metal-semiconductor contacts are simulated with temperature have proven to be in good agreement with the Schottky diodes [17]. $Cu_2ZnSnSe_4$ (CZTSe) thin film has been produced by successfully synthesizing a Au/CZTSe/n-Si/Al heterojunction on silicon substrates for the first time by liquid phase epitaxial growth. It has been shown that heat treatment applied on the CZTSe/n-Si heterojunction device effects the bilateral Schottky diode in such a way that it ensures homogeneous thin-film structures and most importantly stable diode parameters. Dielectric measurements showed that the CZTSe/n-Si heterojunction device is a promising candidate to be used in solar cell applications [18]. Another electrochemical growth study was carried out on a p-Si substrate to produce a Schottky diode from GaTe thin films. A Sn/GaTe based Schottky contact was obtained by evaporation of Sn on a GaTe thin film in high vacuum. The experimental values of the SBH as a function of temperature have been extracted here [19]. Barrier heights of sorbitol doped and non-doped PEDOT:PSS interfacial layer Al/p-Si Schottky contacts were investigated, and it was found that the effective barrier height values increases with organic interlayer modification processes [20]. It has been shown that the fabrication of Gallium nitride Schottky diodes on p-Si is possible by thermal evaporation and synthesizing gallium nitride (GaN) nanoparticles with a chemical sol-gel approach [21].

Schottky diode parameters of Ti/p-strained Si-on-insulator (sSOI), produced by thermionic emission, are strongly dependent on temperature. Looking at the spectral density of the current-noise-power, it was stated that this was due to defects in the Schottky contact depletion region or the presence of traps [22]. Zirconium dioxide-based devices were grown on organic doped glass substrates by sol-gel spin coating system. In the comparative study of zirconium dioxide pure and organic doped Schottky device, it was analyzed that the barrier height, the series resistance, and the ideality factor values decreased due to the doping effect [23]. The effects of Al/(ZnO-PVA)/p-Si based Schottky contacts on radiation were investigated by current-voltage characterization. MPS type Schottky contact parameters in different voltage regions have been declared to cause annealing at high gamma radiation doses exceeding 5 kGy. This result revealed rectifier diode parameters may change in the high electric field region especially interface state density values N_{ss}. Although the diode parameters changed with irradiation, the diode operation remained stable. Al/ZnO-PVA/p-Si SB detectors have been proposed to be promising in different fields due to their low energy consumption utilizing organic/polymer interlayers rather than MIS/-MOS type detectors [24]. The production of Ag/B–Si and Ag/B–Si realized using electrochemical and photo-electrochemical etching, on top of n- and p-type Si/Al contacts is presented. Front contact Ag and back contact Al were deposited by thermal evaporation. A comparison of diode parameters reveals that Schottky diodes in Ag/BS or the binary metal-semiconductor junctions of a diode (Ag/BS/c-Si and c-Si/Al) exhibit almost ideal ohmic properties [25]. A *p*-$CuSbSe_2$ thin film on an n-Si was studied by electron beam deposition. I–V and C–V measurements at different temperatures were applied to evaluate the values of the junction structures such as the ideality factor, built-in voltage, and carrier density. Thermal annealing of the Schottky contact interface of $CuSbSe_2$ also results in significant improvements in diode parameters [26].

In this study, two Cu/p-Si/Al MSM contacts were formed by growing Al and Cu metal contacts on the back and front interface of p-Si substrates using thermal evaporation. The interface states of the Cu/p-Si/Al MSM double SBH at the back Al ohmic and non-ohmic contact, reported in this study, were analyzed utilizing current-voltage (I–V), frequency-dependent capacitance-voltage (C–V), and conductivity-voltage (G-V) characteristics. In this study, the effect of thermal annealing and sample pretreatment on the serial resistance, the ideality factor, the barrier height, and the built-in voltage of the Cu/p-Si/Al MSM double SBH structure have been investigated and optimized resulting in a significant reduction of the SBH. The results of this work play a significant role for an applicaton specific optimization of rectifiying Schottky Barrier Diodes.

2. Methods

Al and Cu thin metal films were grown on the back and front face of p-type Si (100) by thermal evaporation using a Leybold Univex 450 physical vapor deposition system. The boron doped Si wafer with 11.35–2.71 $\times$ 10^{15} cm^{-3} doping concentration used in the study has a crystallographic orientation of (100) and a resistivity of 5–10 Ω-cm. Before the deposition of the contact materials in both of these devices, the Si substrate has been etched with hydrofluoric acid (HF) to remove the native oxide layer formed on the surfaces. The process of obtaining ohmic and non-ohmic samples with Al contact was continued by annealing of Al contact in N_2 inert environment. Next, the Si wafer was rinsed with deionized water in an ultrasonic bath for 30 min and finally cleaned sequentially with methanol and acetone. Afterwards, the substrate has been placed immediately in the physical vapor deposition vacuum system for processing. We commercially obtained high purity Al (99.999%) contact materials with ~500 nm thickness, which has been thermally evaporated in a tungsten boat at a pressure of ~6.1 $\times$ 10^{-6} mbar. Thickness control was performed using a conventional quartz balance during the thermal evaporation process. The layer thickness has been measured afterwards using a scanning electron microscope (SEM, Fig. 1a). The Al contacts have been further prepared by sintering the vaporized Al on the Si back-side for 15 min at 450 °C under N_2 atmospheric pressure to impart ohmic properties to the contact. In Fig. 1a, an SEM cross section of the device is visible showing the back-side of the Si coated with Al that is able to diffuse in N_2 atmosphere at such temperatures. Thus, two ohmic and non-ohmic samples were formed at the rear Al contact part. The non-ohmic sample was kept in the vacuum chamber system. The ohmic contact sample was placed in the thermal evaporation system for Cu contact deposition on the upper surface of both samples. The Cu chosen for the Schottky contact was formed by thermal evaporation in high vacuum at a pressure of ~7.8 10^{-6} mbar. An SEM cross-section micrograph of the p-Si/Cu interface is given in Fig. 1b revealing a thickness of the metal deposited on the Si surface of ~980 nm.

A flow diagram of the double Schottky contact experimental fabrication procedure is given in Fig. 2a. The representation of the energy band diagram of the materials used in the metal-semiconductor-metal contact is given in Fig. 2b. It contributes to our clear understanding of prepared contacts and band structures. The energy levels of each material used are shown here, and two Schottky diodes are obtained by making Cu contacts on the upper side of both samples by applying ohmic and non-ohmic Al contact processes on the back-side of Si wafer.

The current-voltage (*I–V*) characteristics have been measured with the experimental setup shown in Fig. 3. The setup contains a GPIB connection to enable data transfer and acquisition between a Keithley Model 2400 Source Meter Unit (SMU) and a computer. I–V measurement have been recorded using specific Keithley data acquisition software.

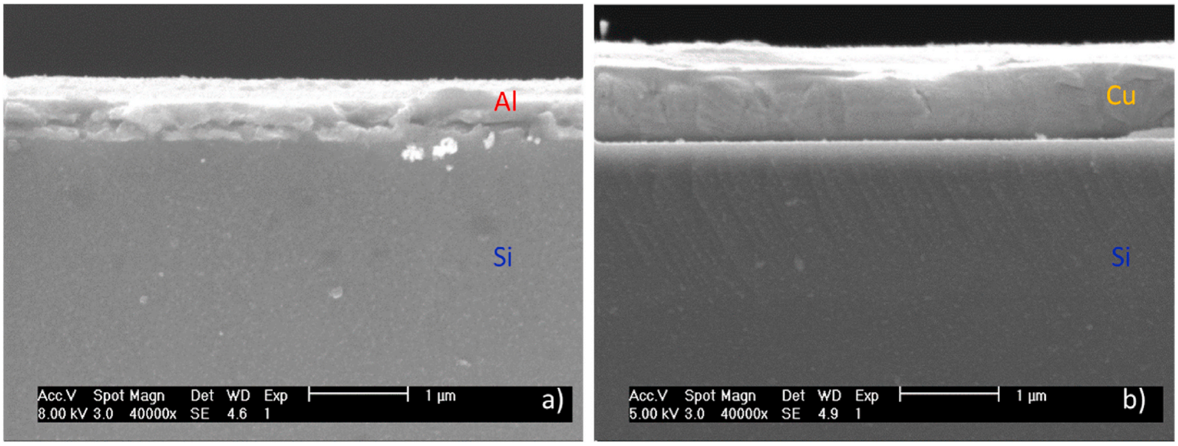

Fig. 1. SEM micrograph of Al/p-Si/Cu Contact; a) Al/p-Si back ohmic contact image, b) Cu/p-Si top Schottky contact image.

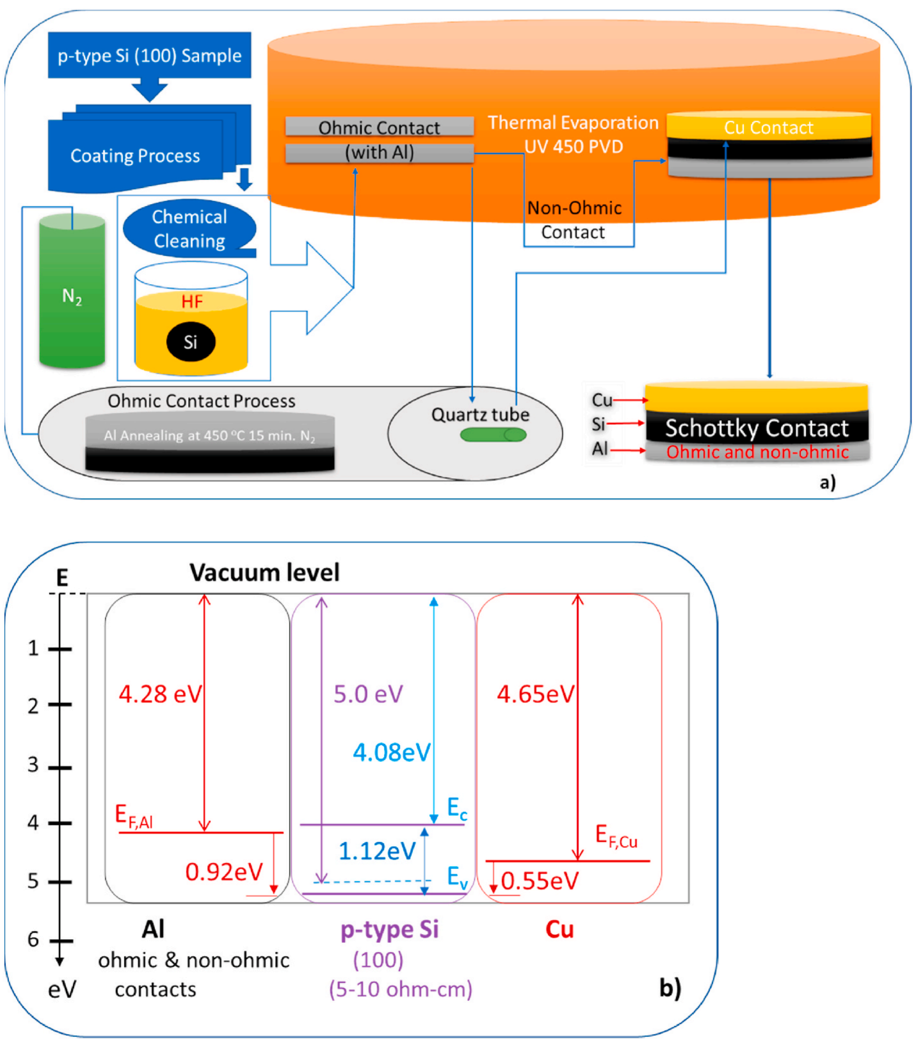

Fig. 2. a) Schottky diode fabrication process scheme; metal (ohmic and non-ohmic) contact/semiconductor/metal contact, b) Energy band diagram of the pre-annealing fabrication of Al/p-Si/Cu double SBH.

Frequency dependent capacitance-voltage (*C–V-f*) and conductance-voltage (G-V-f) measurements have been performed using a HP 4194 A Impedance Analyzer (Fig. 3).

3. Results and discussion

I–V characteristics of the Al/p-Si/Cu MSM/SBH structure for the Al ohmic (450 °C 15 min in N_2 atmosphere) and non-ohmic process are shown in Fig. 4. These graphs show the rectification behavior of both,

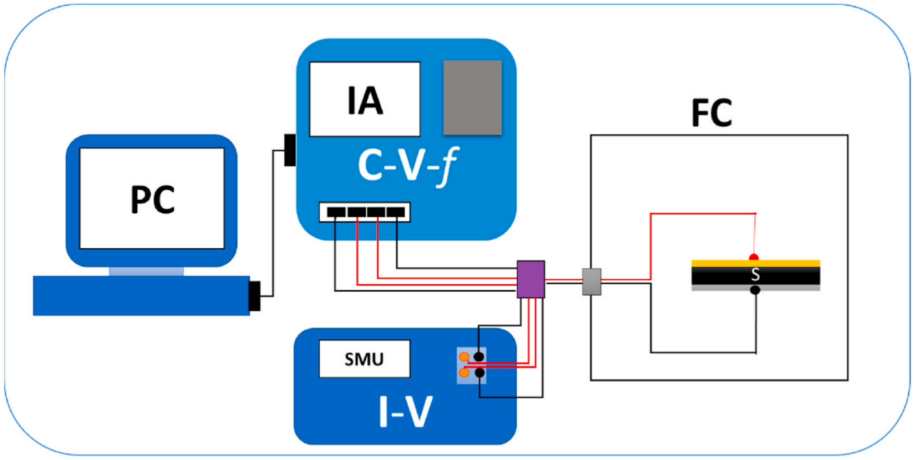

Fig. 3. Experimental setup for the *I–V*, frequency dependent capacitance (*C–V-f*) and conductance (G-*V-f*) in the spot voltage measurements; PC: Computer, IA: Impedance Analyzer, SMU: Source Measurement Unit, FC: Faraday cage, S: Sample.

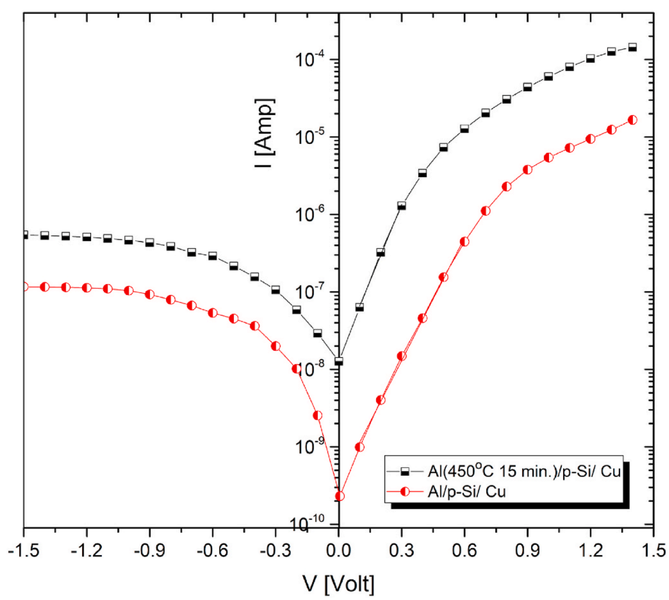

Fig. 4. *I–V* plots of a non-ohmic and ohmic Al (450 °C 15 min. in N_2 atmosphere) contact in an Al/p-Si(100)/Cu SBHs.

ohmic and non-ohmic devices, indicated by a current saturation at reverse bias voltages. The *I–V* characteristics of a MSM Schottky diode in forward bias condition is defined by the following equation [7–10],

$$I = AA^{*}T^{2}\ exp\left(-\frac{q\varnothing_{B}}{kT}\right)exp\left[\left(\frac{qV}{nkT}\right)-1\right] \tag{1}$$

where A is the diode contact area, A^* is the Richardson constant, T is the temperature, k is Boltzmanns constant and φ_B is the SBH. At forward bias voltages exceeding 3kT/q, the equation can be rewritten to Refs. [6,13],

$$I = I_o\ exp\left[\frac{qV}{nkT}\right] \tag{2}$$

where I_o is the saturation current, and n is the ideality factor given by,

$$n = \frac{q}{kT}\frac{dV}{d\ ln\ I} \tag{3}$$

Here, n can be determined from the forward bias current slope in the log *I–V* plot of Fig. 4.

The saturation current is the value at the point that cuts the y-axis at 0 V from the log I–V graph and the barrier height is derived from Eq. (1), respectively, both expression equations are given below [14];

$$I_o = AA^{*}T^{2}\ \exp\left(-\frac{q\varnothing B}{kT}\right) \tag{4a}$$

$$\varphi_B = \frac{kT}{q}ln\left(\frac{AA^{*}T^{2}}{I_o}\right) \tag{4b}$$

Richardson constant A* for p-type Si is 32 A cm^{-2} K^{-2}. The ideality factor of the SBH has been determined from the forward current plot of log I(V) (Fig. 4) and was found to be 1.15 for Al (450 °C 15 min In N_2 atmosphere) and 3.17 for the Al/p-Si(100)/Cu Schottky Diode, respectively. An ideal diffusion current results in $n = 1$, whereas the ideality factor converges to 2 for currents dominated by recombination [14]. The barrier height of SB strongly depends on thermal annealing temperatures and sample treatment as shown in [1] for alternative Co/p-Si Schottky diodes. Here, the SB decreases for temperatures up to 300°C and further increases for temperatures exceeding 300°C up to 600°C. It has been reported, that the passivation effect of the native oxide layer is lost due to annealing and the surface defects change as the Schottky barrier height (SBH) increases at high temperatures [1]. When I_o is determined, φ_B can be obtained using Eq. (4b). Thus, I_o and φ_B can be extracted from the log *I–V* plot. The φ_B value for the diode was found to be 0.48 for Al (450 °C 15 min in N_2 atmosphere) and 0.59 eV for Al/p-Si (100)/Cu Schottky contacts, respectively. Ideality factor values of 1.15 and 3.17 were found for ohmic and non-ohmic Al/p-Si/Cu Schottky contacts, respectively. Since heat treatment has been applied here, it can be concluded that a depletion region disappears between the Si semiconductor and the Al metallic contact. This is demonstrated in Fig. 1a, a cross-sectional SEM image of the metal semiconductor contact, and the Al metal contact diffused.

Cu/p-Si Schottky diode with ohmic contacts obtain a larger saturation current than that of the non-ohmic counterparts. In addition, the results reveal that they exhibit a better rectifier diode behavior. Therefore, there are several effects to consider, along with the ohmic contact factor, causing deviations from an ideal Schottky Diode behavior. Such effects can be annealing, chemical surface cleaning, interface state variations, and the series resistance effect. These diode parameters are important parameters to quantify the Schottky contact performance that itself strongly depends on manufacturing processes.

By investigating the device parameters in more detail, the deviation of the *I–V* characteristics at higher forward current values reveals a downward curvature. In such a case, Cheung's method, which is an alternative technique based on the *I–V* characteristic, can be used to obtain the expressions of the barrier height, the ideality factor, and the series resistance. The equations expressed in terms of Cheung functions are as follows [27],

$$\frac{d\,V}{d\ln I}=n\frac{kT}{q}+IR_s \tag{5a}$$

$$H(I)=V-n\frac{kT}{q}\ln\left(\frac{I}{AA^{*}T^{2}}\right)=n\varnothing_B+IR_s \tag{5b}$$

To obtain the serial resistance R_s, ideality factor n, and barrier heights $\varnothing_B$. The plots of the $(d\,V)/(d\ln I\,)$ and $H(I)$ vs. I of ohmic and non-ohmic Schottky contact have been plotted in Fig. 5a and b. These plots allow precise extraction of n, $\varnothing_B$, and R_s. The n, $\varnothing_B$, and R_s values of the Al ohmic contact were determined from Fig. 5a and found to be 1.155, 0.48 eV and 15.16 Ohm, respectively. The n, $\varnothing_B$, and t R_s values from Fig. 5b were found to be 1.15, 0.59 eV and 187.055 Ohm and correspond to the Al non-ohmic contact. From these parameters, it is obvious that there is a significant performance improvement due to the thermal annealing process of the Al contact since there is a strong decrease in the obtained n, $\varnothing_B$, and R_s values. In this case, the rectifying diode behavior has been significantly improved by at least a factor of ~1.93%. It could be observed that the rectifier diode parameters, here the ideality factor and the built-in voltage values, of the ohmic heterojunction contacts formed by thermal annealing process and the temperature dependent process decreased. These changes are also demonstrated in [8,26] reporting similar studies and improved rectifier diode characteristics due to thermal annealing processes.

The n, $\varnothing_B$, and R_s values extracted from the slope of the I–V curves and obtained by the Cheung method are summarized in Table 1 for each sample. In terms of rectifying properties of Metal-Semiconductor Schottky diodes comprising Al contacts, the results reported in this

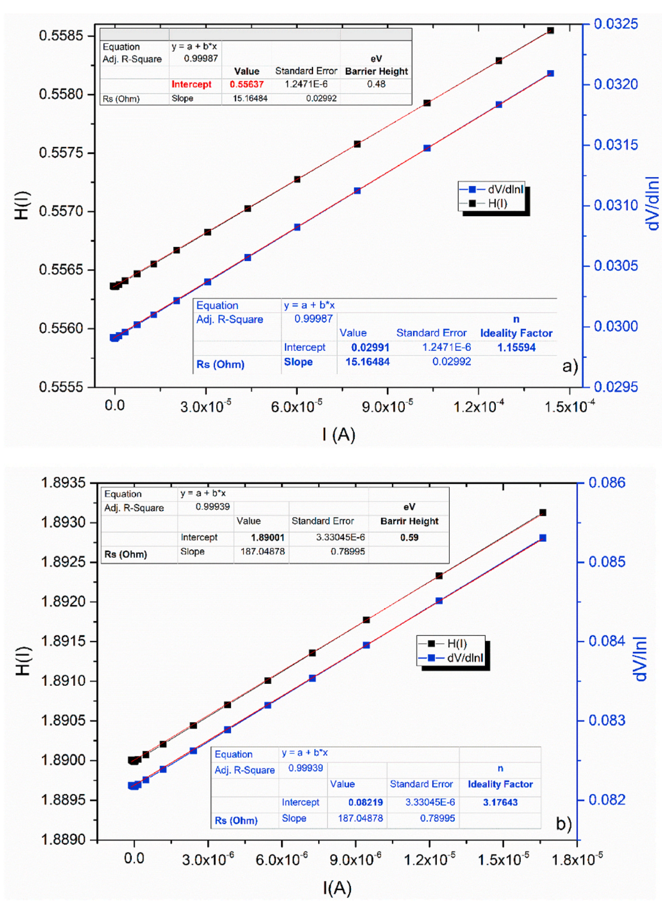

Fig. 5. Plots of $(d\,V)/(d\ln I\,)$ and $H(I)$ vs. I of the Al/p-Si/Cu SBHs; a) ohmic, b) non-ohmic contact.

Table 1
Diode parameters of SBHs (value of 1 mm diameter Cu metal contact).

Parameter	non –ohmic Al/p-Si/Cu	ohmic Al 450 °C, 15 min.N_2/p-Si/Cu
I_o (Amp)	2.32×10^{-10}	1.88×10^{-8}
φ_B (eV)	0.594	0.481
n (I–V)	3.175	1.155
n (H(I)–I)	3.180	1.158
n (dV/d lnI)	3.17	1.15
R_s (I–V) (Ohm)	182.71	17.18
R_s (H(I)–I) (Ohm)	187.05	15.16
R_s (dV/d lnI) (Ohm)	187.05	15.16

work state that significant improvements and better efficiencies were obtained by applying heat treatment on Al contacts.

An effective voltage level change should be investigated by reducing the series resistance value of the rectifier diode connected to the ohmic contact. Depending on the applied voltage, it causes an efficient electron-hole diffusion across the interface layer. To demonstrate this situation, the voltage drop V_i across the interface layer of the derived potential value can be expressed by: [28,29],

$$V_i=\left(1-\frac{1}{n}\right)V \tag{6}$$

Due to this ideality factor, the validity of the voltage drop formula can be applied when the interfacial layer is comparatively thick so that the conductivity between the metal and the semiconductor in the interface layer becomes very small. To reveal the effect of the series resistor R_S, the value of V in Eq. (6) is reformatted by replacing it with V-IR_S. Thus, the formula can be rewritten resulting in the following relation [30],

$$V_i=\left(1-\frac{1}{n}\right)(V-IR_s) \tag{7}$$

The values of V_i were obtained by means of Eq. (7). The voltage obtained from Eq. (6) has to be subtracted from the total value of the applied forward voltage for obtaining a voltage drop across the depletion layer V_D [31],

$$V_D=V-V_i \tag{8}$$

In the following step, the log *I-(V)* curves have been plotted with the obtained V_D and V_i values (Fig. 6a and b) to show the potential influence on a parasitic interface layer by applying the annealing process.

The variation of V_i and V_D reveals important rectifier diode property information in terms of voltage drop across the interfacial layer. Within the ohmic structure, the voltage drop V_D across the interfacial layer of the Schottky Diode is comparatively high as seen in Fig. 6a. In Fig. 6b, it can be seen from the change in V_D that the voltage drop across the interface layer signifiantly decreases and is lower than the V_i voltage values. In addition, a subsequent thermal annealing process on the back Al contact of the p-Si/Cu MS rectifier diode is still required to achieve even better Schottky diode behaviour.

Fig. 7a and b shows the *C–V* plots of the Al/Cu/p-Si Schottky diode at 100 kHz and 1 MHz for the ohmic and non-ohmic contact, respectively. The contact capacitance of a Schottky metal semiconductor contact area in the depletion region can be expressed as [14,15],

$$\frac{1}{C^2}=\frac{2(V_{bi}+V)}{A^2\varepsilon_s qN_a} \tag{9}$$

where V_{bi} is the built-in potential, ε_s is the dielectric constant of semiconductor and N_a is the doping concentration. Plotting C^{-2} *vs.* V results in a straight line allows us to extract the build-in potential and doping concentration of the structure (Fig. 7c and d).

The linearity in the C^{-2} vs. V plot is indicating that the charge carrier density within the depletion region of the diode is uniform. The model of

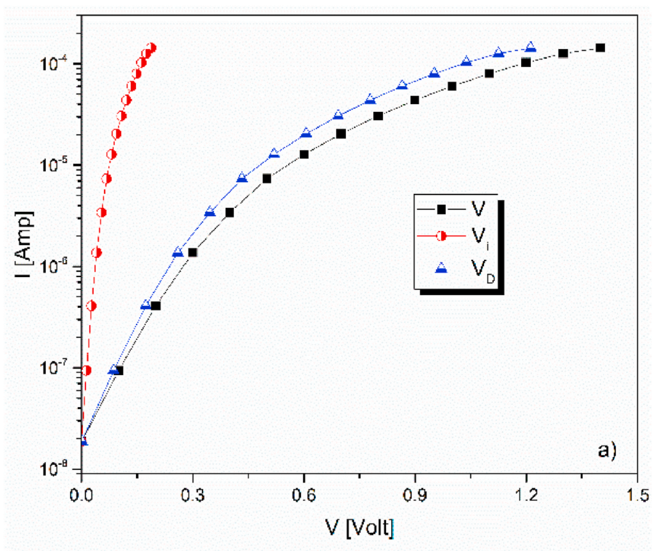

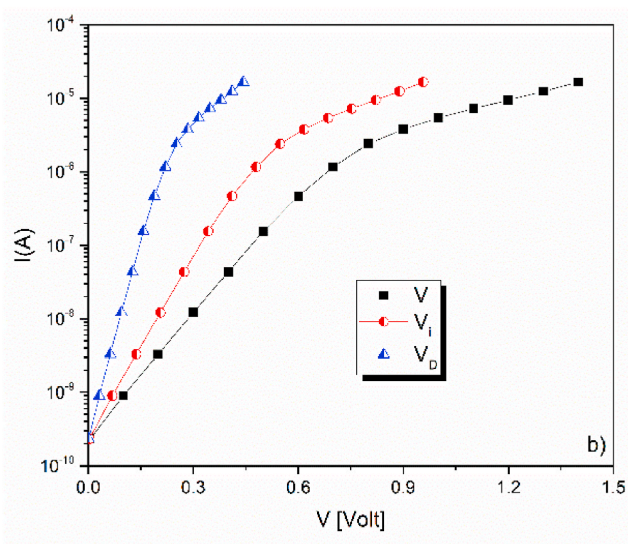

Fig. 6. V, V_i and V_D vs. forward current values of Al/p-Si/Cu SBHs; a) ohmic, b) non-ohmic contact.

this change [14,16]; in the case of double Schottky Diode between p-Si and Cu metal contact, the acceptors evenly distributed in the p-Si are compensated by electrons transferred from the metal until equilibrium. Therefore, a Schottky contact depletion region is created within the interface layer. In the depletion region, electrons are trapped in the acceptors to form negative space charges that are considered to be uniformly distributed. The linearity in the C^{-2}-V curves can be explained by free carriers. The linear variation obtained is due to the uniform distribution of the interfacial state density N_{SS} and the doping concentration N_a in the band gap. The capacitance at higher frequencies does not depend on the voltage, indicating that the capacitance at higher frequencies is not a result of the variation in surface charges. The values of V_{bi} and N_a can be obtained from the intercept and slope of C^{-2} *vs. V* plot by means of Eq. (10) and 11, respectively. The doping concentration N_a and the built-in potential V_{bi} values were found to be for the ohmic Schottky contact 8.022×10^{14} cm^{-3}, 6.15×10^{14} cm^{-3} and 0.33eV, 0.16 eV of the spot frequency 100 kHz and 1 MHz, respectively. These values were found to be for the non-ohmic Schottky contact 6.952×10^{13} cm^{-3}, 4.102×10^{13} cm^{-3} and 0.58eV, 0.37 eV for the spot frequencies 100 kHz and 1 MHz with an adjusted R-square value 0.9986 of the plot, respectively. The barrier height value V_{bi} of the metal-semiconductor Schottky contact can be expressed by [30,31],

$$\varnothing_B = V_{bi} + V_p + \frac{kT}{q} \tag{10}$$

with

$$V_p = \frac{kT}{q} ln\left(\frac{N_V}{N_a}\right) \tag{11a}$$

with the effective charge carrier density $N_v = 1.83 \times 10^{19}$ cm^{-3} [32]. From these equations, the barrier height φ_B was found to be 0.61eV and 0.45 eV for spot frequencies of 100 kHz and 1 MHz for the ohmic Schottky contact, respectively. For the non-ohmic contact, the SBH has been determined to be 0.92eV and 0.73 eV for spot frequencies of 100 kHz and 1 MHz, respectively. From the experimental results it can be derived that the barrier height φ_B obtained from the *C–V* curve is higher than φ_B derived from the *I–V* measurements. This discrepancy is probably due to existence of an interfacial layer. These results are in very good agreement with other studies reported in Refs. [33,34]. A summary of the built-in potential V_{bi}, band gap density N_a, and barrier height values φ_B extracted by frequency-dependent *C–V* measurements are given in Table 2.

It has been observed that the rectifier diode parameters, especially the ideality factor and the built-in voltage values, of the ohmic heterojunction contacts formed by the thermal annealing process decreased significantly.

Besides key figures of merit, interface states can further be extracted from frequency dependent *C–V* and *G-V* measurements. Here, C_{SS} is the capacitance, and G_{SS} is the conductance for the metal-semiconductor (MS) structure that can be expressed by Ref. [35],

$$C_{ss} = \frac{AqN_{ss}}{\omega\tau} \mathrm{arctg}(\omega\tau) \tag{11b}$$

$$G_{ss} = \frac{AqN_{ss}}{2\tau} ln\left(1+\omega^2\tau^2\right) \tag{12}$$

where N_{SS} is the density of interface states, τ is the relaxation time constant, and ω is the angular frequency of the interface states. Fig. 8 shows C-*f* curves of Cu/p-type Si Schottky contact at various spot bias voltages.

As shown in Fig. 8, the interfacial capacitance values decrease with increasing angular frequency and remain almost constant towards higher frequencies. The decrease of the capacitance in the frequency domain with the applied bias voltages, results in a change in the symmetry due to the penetration of the electrical field across the interface layer. Depending on the interface states at low frequencies, it follows the alternating current (AC) signal and reveals the rectification property of the Schottky diode. At high frequencies, however, the interface states reach a constant value at each supply voltage and cannot follow AC signals. Thus, it shows that the contribution of the interfacial state capacitance to the total capacitance is negligible [36]. As shown in the figure, the capacitance obtains a saturation at a certain angular frequency value. When the traps start to respond to the signal, the capacitance values decrease with increasing angular frequency. However, at high angular frequencies in this Schottky diode structure, the traps no longer respond.

As shown in Fig. 9, the density of the interface states and the time constant of the traps were calculated by fitting with Eq. (12) and by deriving the frequency dependent conductivity for the Al (450 °C 15 min)/p-type Si/Cu Schottky Diode. These values are given in Table 3. As seen in the figure, there are two regions with alternating segments in the low frequency and high frequency regions. In both of these regions, the AC conductivity increases with increasing frequency and the conductivity value decreases symmetrically with the bias voltage in both regions. The second region is considered to be a bypass feature of carriers trapped between the full and empty states at the Fermi level. Atoms

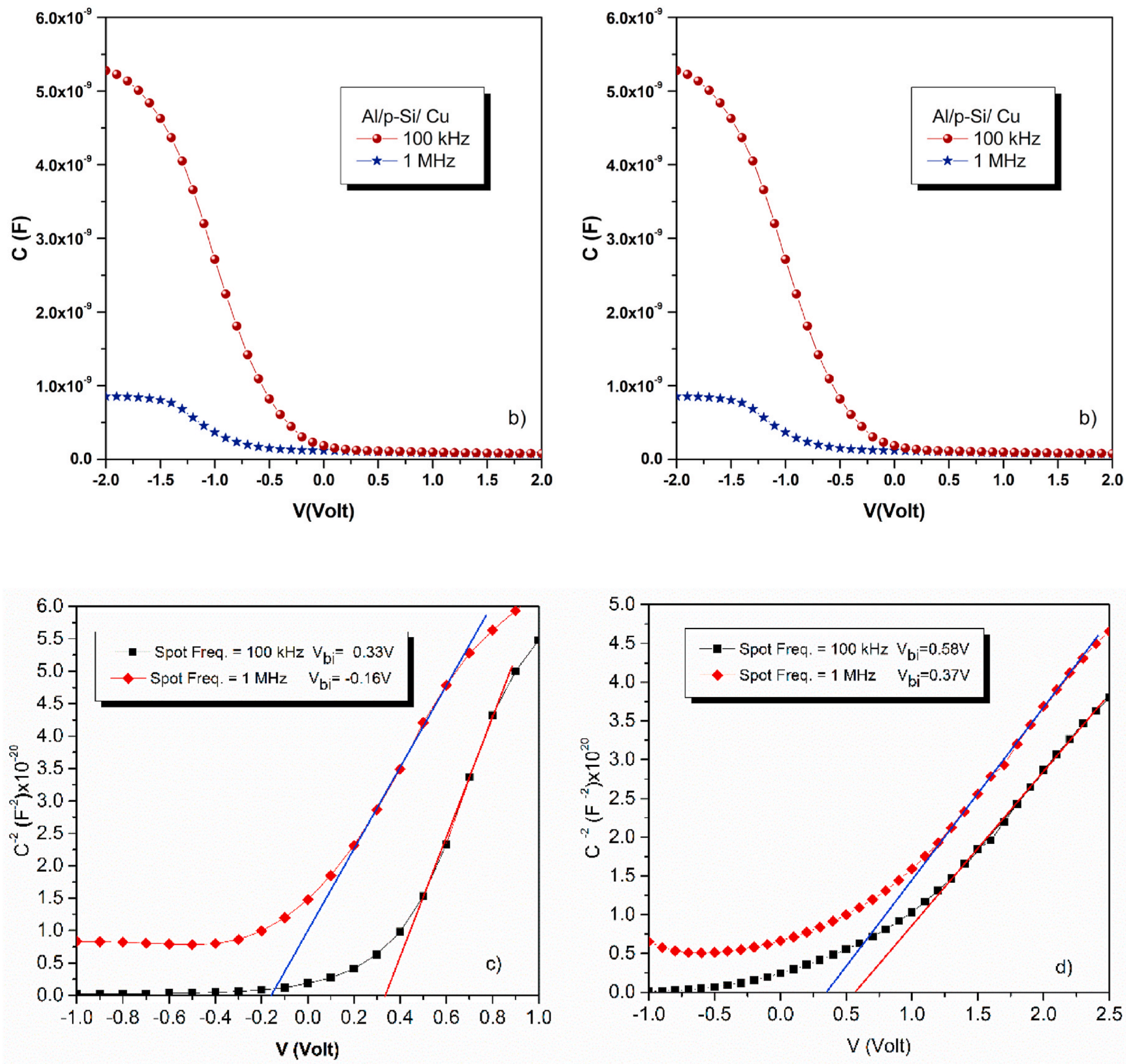

Fig. 7. *C–V*; a) ohmic, b) non-ohmic contact, and C^{-2}-*V*; c) ohmic, d) non-ohmic contact plots of Al/p-Si/Cu SBHs.

Table 2
V_{bi}, N_a, φ_B parameters derived by *C–V* technique of Al/p-Si/Cu SBHs.

Sample	V_{bi}		N_a		φ_B	
	100 kHz	1 MHz	100 kHz	1 MHz	100 kHz	1 MHz
Al/p-Si/Cu	0.58	0.37	6.95E13	4.10E13	0.92	0.73
Al (450°C15 min)/p-Si/Cu	0.33	0.16	8.02E14	6.15E14	0.61	0.45

incorporated in the thin interlayer at the metal-semiconductor contact interface act as additional impurities in the disordered layer. Thus, the transmission mechanism takes place across this layer and can be expressed by Ref. [36],

$$G(\omega)\propto\omega^{p} \tag{13}$$

where *p* is a constant, which is a measure of the amount of charge carriers [37].

The value *p* is derived from the slope of the second region at higher frequencies and it is found to be 0.60–0.64. The *p* values suggest that 60–64% of traps are empty and therefore corresponds to a trap filling probability that changes with the applied electrical field [37].

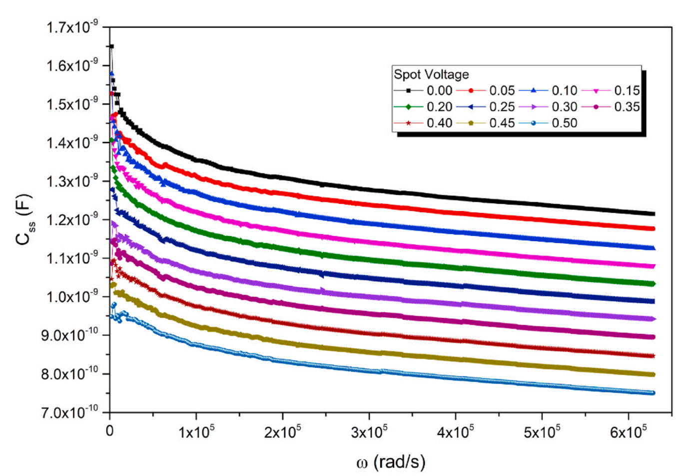

Fig. 8. Frequency dependency capacitance plot at various spot voltages of Al (450 °C 15 min)/p-Si/Cu SBH.

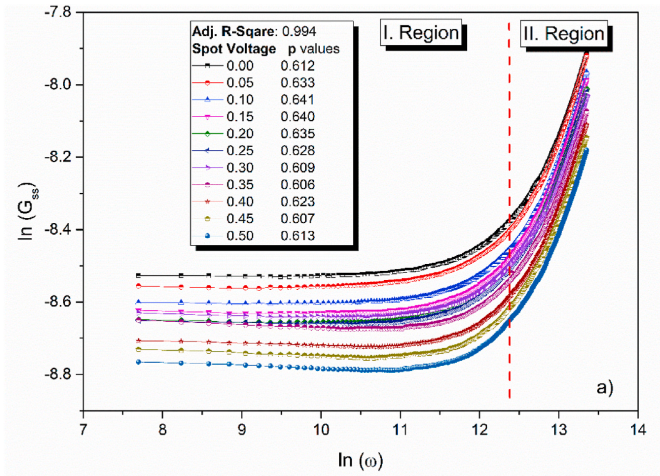

Fig. 9. Variation of the conductance with respect to frequency for Al (450 °C 15 min)/p-Si/Cu SBH.

Table 3
The interfaces parameters of Al/p-Si/Cu SBH.

V_s(V)	E_{SS}-E_V (eV) 100 kHz	E_{SS}-E_V (eV) 1 MHz	N_{ss} (eV^{-1} cm^{-2})	τ (s)
0.00	0.62	0.45	1.08E14	1.16E-6
0.05	0.57	0.40	1.05E14	1.14E-6
0.10	0.52	0.35	1.01E14	1.22E-6
0.15	0.47	0.30	9.74E13	1.23E-6
0.20	0.42	0.25	9.36E13	1.25E-6
0.25	0.37	0.20	8.94E13	1.26E-6
0.30	0.32	0.15	8.51E13	1.27E-6
0.35	0.27	0.10	8.18E13	1.28E-6
0.40	0.22	0.05	7.78E13	1.33E-6
0.45	0.17	0.002	7.38E13	1.35E-6
0.50	0.12	−0.047	6.99E13	1.39E-6

As shown in figures, Eq. (11) can be applied to obtain interface parameters. The interface density and time constant are obtained from the maxima of the C_{SS}-ω curves as shown in Fig. 7. The values of N_{SS} and τ have also been calculated and are summarized in Table 3. In a p-type metal-semiconductor, the energy of the interface states E_{SS} with respect to the top of the valence band at the surface of semiconductor is described as [38],

$$E_{ss} - E_V = q\varnothing_B - qV \tag{14}$$

where E_{SS} is the energy of interface states and E_V is the valence band edge. E_{SS}-E_V values were determined using Eq. (14) and are given in Table 3.

Variation of N_{SS} as a function of the applied voltage for the Schottky diode is shown in Fig. 10. The interface state density N_{SS} here exhibits a linear decrease with the applied bias voltage where each value corresponds to a position within the p-Si gap. This interface state density shows the characteristics of a Schottky rectifier diode with unidirectional conduction mechanism by responding to the forward voltage. The electron-hole transfer mechanism was thus demonstrated by linearly decreasing the interface state density in the interface layer with increasing feedforward voltage.

4. Conclusions

Two structures containing Al contacts format the back-side of a p-type Si wafer were formed by thermal evaporation prior to native oxide layer removal using hydrofluoric acid. By applying thermal annealing at 450°C for 15 minutes, ohmic and non-ohmic Al contacts were formed resulting in, Al/p-Si/Cu dual Schottky barrier diodes. The electronic

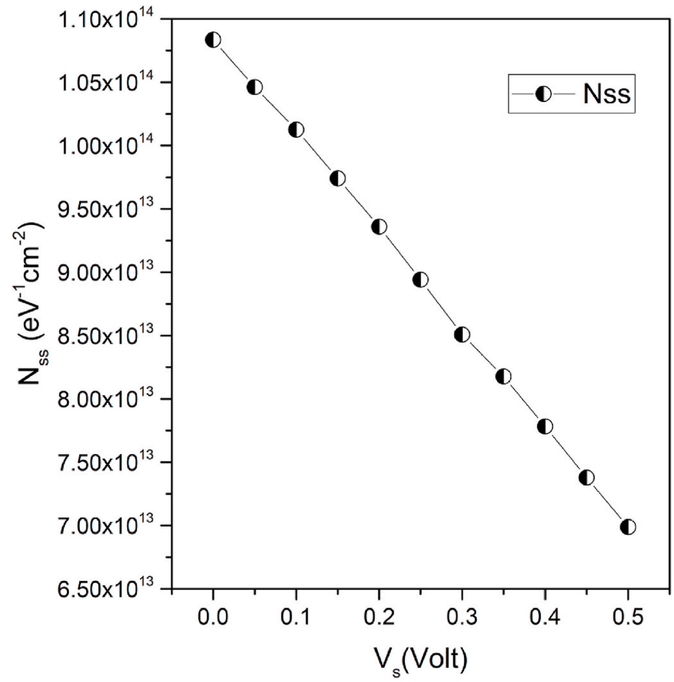

Fig. 10. Interface state density N_{SS} as a function of the applied bias voltage for Al (450 °C 15 min)/p-Si/Cu SBH.

energy and interfacial state density distribution properties of this dual SBH structures were investigated and it was revealed that the ideal distribution exhibited better rectifier diode properties in the ohmic contact applied structure. Interface state density N_{SS} and relaxation time τ of MSM SBH were determined by frequency dependent *C–V* and *G-V* methods. The obtained results show that the thermal annealing applied on the ohmic contact process improves the rectifier diode behaviour of the metal-semiconductor-metal (MSM) structure. The rectifying diode parameters such as diode ideality factor, barrier height and serial resistance parameters were found to be 1.15, $\varphi_{B(I-V)} = 0.48$ eV ($\varphi_{B(C-V)} = 0.61$ eV in 100 kHz), and 17.18 Ω for the ohmic and 3.17, $\varphi_{B(I-V)} = 0.59$ eV ($\varphi_{B(C-V)} = 0.92$ eV in 100 kHz), and 182.71 Ω for the non-ohmic SBH, respectively. The frequency dependent diode parameters of the ohmic contact SBH are lower than that of the non-ohmic contact SBH counterpart. It has been shown that ohmic contact processing, precisely a thermal post annealing at 450 °C for 15 min in this specific case, plays an important role in the emergence of optimized Al/p- Si/Cu SBH for rectifying diode applications for numerous implementations. This result shows that the Al-ohmic contact Schottky contact will be a potential candidate for rectifier diode applications by obtaining high current and low resistance condition at forward bias voltages.

Credit author statement

Mustafa Okutan (MO): Methodology, Investigation, Conceptualization, Writing-review & editing. **Andreas Bablich (AB):** Investigation, Visualization, Writing-review & editing. **Peter Haring Bolivar (PHB):** Validation, Data curation, Writing-review & editing.

Declaration of competing interest

The authors declare the following financial interests/personal relationships which may be considered as potential competing interests:

Mustafa Okutan reports equipment or supplies was provided by University of Siegen.

Data availability

The authors are unable or have chosen not to specify which data has been used.

References

[1] G. Güler, S. Karataş, O.F. Bakkaloğlu, Annealing temperature effect on electrical characteristics of Co/p-type Si Schottky barrier diodes, Phys. B Condens. Matter 404 (8–11) (2009) 1494–1497.

[2] I.M. El Radaf, Mahmoud Nasr, A.M. Mansour, Structural, electrical and photovoltaic properties of CoS/Si heterojunction prepared by spray pyrolysis, Mater. Res. Express (2018), https://doi.org/10.1088/2053-1591/aaa25e, 5-1.

[3] M.J. Yun, D. Lee, S. Kim, C. Wenger, H.D. Kim, A nonlinear resistive switching behaviors of Ni/HfO_2/TiN memory structures for self-rectifying resistive switching memory, Mater. Char. 182 (2021), 111578.

[4] J.M. Dhimmar, H.N. Desai, B.P. Modi, The effect of interface states density distribution and series resistance on electrical behaviour of Schottky diode, Mater. Today Proc. 3 (6) (2016) 1658–1665.

[5] Y. Li, L. Fu, J. Sun, X. Wang, Study of barrier height and trap centers of Au/n-$Hg_3In_2Te_6$ Schottky contacts by current-voltage (I-V) characteristics and deep level transient spectroscopy, J. Appl. Phys. 117 (2015), 085704.

[6] S.K. Tripathi, M. Sharma, Analysis of the forward and reverse bias I-V and C-V characteristics on Al/PVA: n-PbSe polymer nanocomposites Schottky diode, J. Appl. Phys. 111 (2012), 074513.

[7] G. Çankaya, N. Uçar, Schottky barrier height dependence on the metal work function for p-type Si Schottky diodes, Zeitschrift fur Naturforschung Section A-A Journal of Physical Sciences 59 (11) (2004) 795–798.

[8] M. Nasr, I.M. El Radaf, A.M. Mansour, Current transport and capacitance–voltage characteristics of an n-PbTe/p-GaP heterojunction prepared using the electron beam deposition technique, J. Phys. Chem. Solid. 115 (2018) 283–288, https://doi.org/10.1016/j.jpcs.2017.12.029.

[9] L.S. Chuah, Z. Hassan, H. Abu Hassan, Red light emitting Schottky diodes on p-type GaN/AlN/Si(111) substrate, Int. J. Mod. Phys. B 24 (9) (2010) 1129–1135.

[10] A.A. Al-Ghamdi, O.A. Al-Hartomy, F. Yakuphanoglu, Modification of interface states and series resistance properties of Al/p-type Si Schottky diode with HF chemical treatment, Optoelectronics and Advanced Materials-Rapid Communications 6 (1–2) (2012) 292–295.

[11] S. Zeyrek, E. Acaroğlu, M.M. Bübül, The effect of series resistance and interface states on the frequency dependent C-V and G/w-V characteristics of Al/perylene/p-Si MPS type Schottky barrier diodes, Curr. Appl. Phys. 13 (7) (2013) 1225–1230.

[12] P.L. Hanselaer, W.H. Laflére, R.L. Van Meirhaeghe, F. Cardon, Current-voltage characteristic of Ti-pSi metal-oxide-semiconductor diodes, J. Appl. Phys. 56 (1984) 2309.

[13] D.U. Lootens, P.L. Hanselaer, W.H. Laflère, R.L. Van Meirhaeghe, F. Cardon, On the temperature dependence of the Mott–Schottky characteristics of high-barrier Ti–p-Si metal-insulator-semiconductor diodes, J. Appl. Phys. 61 (1987) 2277, https://doi.org/10.1063/1.337990.

[14] S.M. Sze, K.K. Ng, Physics of Semiconductor Devices, third ed., Wiley, 2006, ISBN 978-0-470-06832-8.

[15] E.H. Rhoderick, R.H. Williams, Metal–Semiconductor Contacts, second ed., Oxford University Press, Oxford, New York, 1988.

[16] R. Boumaraf, N. Sengouga, M. Henini, Deep traps and temperature effects on the capacitance of p-type Si-doped GaAs Schottky diodes on (211) and (311) oriented GaAs substrates, Superlattice. Microst. 65 (2014) 319–331.

[17] N. Sengouga, R. Boumaraf, M. Henini, Modeling the effect of deep traps on the capacitance-voltage characteristics of p-type Si-doped GaAs Schottky diodes grown on high index GaAs substrates, Mater. Sci. Semicond. Process. 36 (2015) 156–161.

[18] A. Ashery, I.M. El Radaf, Mohamed M.M. Elnasharty, Electrical and dielectric characterizations of Cu2ZnSnSe4/n-Si heterojunction, Silicon 11 (2019) 2567–2574, https://doi.org/10.1007/s12633-018-0047-2.

[19] K. Cinar, Z. Caldiran, S. Aydogan, Electrochemical growth of GaTe onto the p-type Si substrate and the characterization of the Sn/GaTe Schottky diode as a function of temperature, Thin Solid Films 550 (2014) 40–45.

[20] V. Janardhanam, H.J. Yun, C.J. Choi, Energy-level alignment and electrical properties of Al/p-type Si Schottky diodes with sorbitol-doped PEDOT: PSS as an organic interlayer, J. Alloys Compd. 637 (2015) 84–89.

[21] F. Yakuphanoglu, F.S. Shokr, F. El-Tantawy, A new type photodiode: p-Si/GaN pn junction in series with GaN/Ag Schottky diode, J. Alloys Compd. 650 (2015) 671–675.

[22] I. Jyothi, H.K. Lee, C.J. Choi, Double barrier height nature of Ti/p-Type strained Si-On-Insulator Schottky diode and its low frequency noise characteristics, J. Nanosci. Nanotechnol. 17–10 (2017) 7107–7114.

[23] K. Sasikumar, R. Bharathikannan, M. Raja, Effect of organic additives on the characteristics of Al/organic additive: ZrO_2/p-Si metal-insulator-semiconductor (MIS) type Schottky barrier diodes, J. Inorg. Organomet. Polym. Mater. 30–2 (2020) 564–572.

[24] A. Kaymaz, E.E. Baydilli, Y. Azizian-Kalandaragh, Evaluation of gamma-irradiation effects on the electrical properties of Al/(ZnO-PVA)/p-Si type Schottky diodes using current-voltage measurements, Radiat. Phys. Chem. 183 (2021), 109430.

[25] H.M. Hwail, M. Midhat, A comparative study of two types of substrates in the manufacture of Schottky diode: p-Si and n- Si, Int. J. Nonlinear Anal. Appl. 13 (1) (2022) 1303–1310.

[26] I.M. El Radaf, M.S. El-Bana, Synthesis and characterization of the $CuSbSe_2$/n-Si heterojunction: electrical and photovoltaic characterizations, Phys. B Condens. Matter 584 (2020), 412067, https://doi.org/10.1016/j.physb.2020.412067.

[27] S.K. Cheung, N.W. Cheung, Extraction of Schottky diode parameters from forward current-voltage characteristics, Appl. Phys. Lett. 49 (1986) 85.

[28] H.C. Card, E.H. Rhoderick, Studies of tunnel MOS diodes I. Interface effects in silicon Schottky diodes, J. Phys. D 4 (1971) 1589.

[29] C.Y. Wu, Interfacial layer theory of the Schottky barrier diodes, J. Appl. Phys. 51 (1980) 3786.

[30] E. Ayyıldız, A. Türüt, H. Efeoğlu, S. Tüzemen, M. Sağlam, Y.K. Yoğurtçu, Effect of series resistance on the forward current-voltage characteristics of Schottky diodes in the presence of interfacial layer, Solid State Electron. 39 (1996) 83.

[31] M. Sochacki, A. Kolendo, J. Szmidt, A. Werbowy, Properties of Pt/4H-SiC Schottky diodes with interfacial layer at elevated temperatures, Solid State Electron. 49 (2005) 585.

[32] M. Çakar, C. Temirci, A. Türüt, Determination of the density distribution of interface states from high-and low-frequency capacitance characteristics of the tin/organic pyronine-B/p-type silicon structure, ChemPhysChem 3 (8) (2002) 701–704.

[33] J.P. Sullivan, R.T. Tung, M.R. Pinto, W.R. Graham, Electron transport of inhomogeneous Schottky barriers: a numerical study, J. Appl. Phys. 70 (1991) 7403.

[34] A. Türüt, N. Yalçın, M. Sağlam, Parameter extraction from non-ideal C-V characteristics of a Schottky diode with and without interfacial layer, Solid State Electron. 35 (1992) 835–841.

[35] E.H. Nicollian, A. Goetzberger, The Si-SiO_2 interface-electrical properties as determined by the metal-insulator-silicon conductance technique, Bell. Syst. Rech. J. 46 (6) (1967) 1055–1133.

[36] B. Akkal, Z. Benamara, B. Gruzza, L. Bideux, Characterization of interface states at Au/InSb/InP(100) Schottky barrier diodes as a function of frequency, Vacuum 57 (2000) 219–228.

[37] J.C. Dyre, T.B. Schrøder, Universality of ac conduction in disordered solids, Rev. Mod. Phys. 72 (2000) 873.

[38] B. Akkal, Z. Benamara, L. Bideux, B. Gruzza, Electrical characterization of the Au/InP(100) and Au/InSb/InP(100) structures, Microelectron. J. 30 (7) (1999) 673–678.